Proceedings of ASME Turbo Expo 2011
GT2011
June 6-10, 2011, Vancouver, British Columbia, Canada

GT2011-46115

COMPARISON BETWEEN SELF-EXCITED AND FORCED FLAME RESPONSE OF AN INDUSTRIAL LEAN PREMIXED GAS TURBINE INJECTOR

Stephen Peluso, Bryan D. Quay, Jong Guen Lee, Domenic A. Santavicca
Department of Mechanical and Nuclear Engineering
Center for Advanced Power Generation
The Pennsylvania State University, University Park, PA, 16802

ABSTRACT

An experimental study was conducted to compare the relationship between self-excited and forced flame response in a variable-length lean premixed gas turbine (LPGT) research combustor with a single industrial injector. The variable-length combustor was used to determine the range of preferred instability frequencies for a given operating condition. Flame stability was classified based on combustor dynamic pressure measurements. Particle velocity perturbations in the injector barrel were calculated from additional dynamic pressure measurements using the two-microphone technique. Global CH* chemiluminescence emission was used as a marker for heat release. The flame's response (i.e. normalized heat release fluctuation divided by normalized velocity fluctuation) was characterized during self-excited instabilities. The variable-length combustor was then used to tune the system to produce a stable flame at the same operating condition and velocity perturbations of varying magnitudes were generated using an upstream air-fuel mixture siren. Heat release perturbations were measured and the flame transfer function was calculated as a function of inlet velocity perturbation magnitude. For cases in this study, the gain and phase between velocity and heat release perturbations agreed for both self-excited and forced measurements in the linear and nonlinear flame response regimes, validating the use of forcing measurements to measure flame response to velocity perturbations. Analysis of the self-excited flame response indicates the saturation mechanism responsible for finite limit amplitude perturbations may result from nonlinear driving or damping processes in the combustor.

NOMENCLATURE

a	slope
A	velocity perturbation amplitude
CH^*	CH* chemiluminescence emission
f	frequency
Δf	frequency resolution
FTF	flame transfer function
G_{xx}	single-sided power spectral density
i	frequency bin number
L_C	combustor length
N	number of data points
m	mass
P, p	pressure
Q, q	heat release
R^2	coefficient of determination
rms	root mean squared quantity
V, v	particle velocity
x	parameter

GREEK LETTERS

ρ	density
σ	absolute uncertainty
θ	phase difference

OVERSCRIPTS AND SUPERSCRIPTS

‘	fluctuating quantity
·	time rate of change

SUBSCRIPTS

COMB	combustor
FUEL	fuel
FUNDAMENTAL	fundamental frequency
IN	inlet
LC	limit cycle
MEAN	time-averaged
RMS	root mean square

Copyright © 2011 by ASME

INTRODUCTION

Gas turbines operating on natural gas produced approximately twenty-one percent of all electrical energy in the United States in 2008 [1]. Industrial gas turbines occupy a unique role in electrical production; they are used primarily in peaking power plants due to the ability to adjust output quickly to match demand [2]. Almost all other power production methods provide base load power production due to limited response ability. Even with an increased focus on nuclear and renewable energy in the United States over the next few decades, gas turbines will remain a vital component of electrical energy production [3].

Early conventional gas turbines used diffusion flame combustors resulting in reliable performance and high stability. Unfortunately, diffusion flames generate high reaction zone temperatures which result in elevated thermal nitric oxides (NO_x) production. Starting in the mid-1980s, emission limits lead to the development of dry low NO_x lean premixed gas turbines (LPGT). Lean premixed combustion reduces the reaction zone temperature, limiting thermal NO_x production and emission. Current low NO_x systems without additional exhaust gas treatment are capable of achieving less than 9 ppmv NO_x in the exhaust at 15% excess oxygen. This represents a significant improvement over conventional combustors which typically produce several hundred ppmv NO_x [4].

Unfortunately, lean-premixed combustion systems are vulnerable to combustion instabilities. Combustion instabilities are high amplitude oscillations sustained by coupling between flame heat release and system acoustics. They are self-excited oscillations, involving complex interaction between the acoustic pressure field, particle velocity field, local flame heat release, and system boundaries. Particle velocity is a macroscopic property of a theoretical fluid element, not to be confused with the phase speed of a pressure fluctuation (speed of sound). Fluid elements are an infinitesimal small collection of a sufficient number of molecules to ensure acoustic variables (pressure, density, and other thermodynamic properties) are uniform throughout the element. While the actual velocity of any individual molecule within the element is seemingly random, particle velocity represents the effect of acoustic pressure waves on the motion of a fluid element [5]. Large instabilities can cause flame flashback, blow-off, and increase vibration which can result in structural damage to the turbine.

Lean premixed gas turbines are particularly sensitive to combustion instabilities for multiple reasons. The equivalence ratio of the flame is typically close to the lean blowout limit to reduce flame temperature. During unstable combustion, the equivalence ratio of the reactants can fluctuate due to coupling between the fuel delivery system and pressure oscillations in the combustor. If the equivalence ratio drops below the lean blowout limit, the flame will extinguish. Once the equivalence ratio increases above the lean blowout limit the flame can reignite, generating large variations in heat release [6]. Flames in LPGT are typically short compared to longitudinal acoustic wavelengths and can be considered acoustically compact, allowing for easy coupling between heat release and system acoustics [7]. Earlier conventional diffusion flame combustors typically supplied secondary dilution or film cooling air through the liner to reduce the temperature of combustion products and protect the liner wall. These liners contained many small apertures that acted as acoustic attenuators, dampening resonant pressure fluctuations in the combustor. Current premixed combustors used limited secondary air, reducing the dampening effects present in older conventional systems [8].

Combustion Instability Description

The feedback process necessary to sustain unstable combustion is shown in Fig. 1. The overall process is divided into three steps: (1) heat release oscillations generate acoustic pressure oscillations, (2) acoustic pressure oscillations generate velocity or equivalence ratio oscillations, and (3) velocity or equivalence ratio oscillations generate heat release oscillations, completing the feedback cycle.

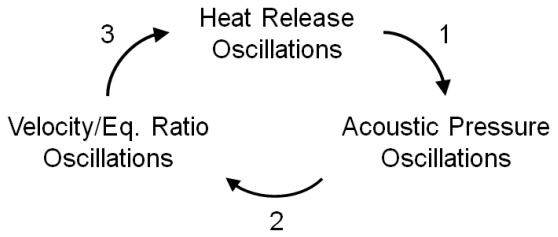

Figure 1. Instability process description (modified from [9]).

In order for unstable combustion to be maintained, a perturbation in heat release must positively couple with the acoustic pressure field in the combustor (step 1). Lord Rayleigh first proposed the correct conditions for coupling during the mid-1870s. Energy is added to the acoustic field if the heat release perturbation is in phase with pressure perturbations in the gas. Conversely, energy is removed from the acoustic field if the heat release and pressure perturbations are out of phase [10].

The phase difference θ between heat release q and acoustic pressure p quantifies Rayleigh's criterion:

$0° < |\theta_{p-q}| < 90°$ energy added to acoustic field
$90° < |\theta_{p-q}| < 180°$ energy removed from acoustic field

Satisfaction of Rayleigh's criterion is necessary for sustaining unstable combustion, but not sufficient. Acoustic pressure perturbations generated by heat release perturbations must couple with other fluid properties in the combustor to sustain the feedback cycle (step 2). The fluid properties of most importance in the feedback cycle are particle velocity and equivalence ratio as they directly relate to the fuel flow rate into the flame. In perfectly premixed systems, acoustic pressure

Copyright © 2011 by ASME

perturbations generate particle velocity perturbations, modulating the mixture mass flow rate. However, most industrial combustion systems operate in partially premixed (also called technically premixed) mode where fuel is injected a short distance upstream of the flame. In these systems acoustic pressure perturbations may generate both velocity and equivalence ratio perturbations.

Flame Response Description

The last relationship necessary to complete the feedback cycle is the heat release response of the flame to velocity and/or equivalence ratio perturbations (step 3). Inlet perturbations may be amplified or damped by the flame, depending on flame configuration and operating condition. Global heat release response can be characterized using a flame transfer function (FTF). The flame transfer function is a construct used to quantify the relationship between overall heat release from a flame subject to oscillations in mixture velocity and/or equivalence ratio. This study focuses on the heat release response of premixed flames to velocity oscillations. Fuel and air are well mixed upstream of a choking plate to ensure a mixture with a temporally constant and spatially uniform equivalence ratio. For a premixed flame the flame transfer function directly relates the normalized velocity and heat release oscillation amplitudes (Eq. 1):

$$FTF(f,A) = \frac{\dot{Q}'(f)/\dot{Q}_{MEAN}}{V'(f)/V_{MEAN}} \qquad (1)$$

where $\dot{Q}_{MEAN}$ is the time-averaged heat release rate from the flame, V_{MEAN} is the mean velocity in the injector barrel, and $\dot{Q}'$ and $\dot{V}'$ are the frequency dependent complex fluctuation amplitudes of heat release and velocity respectively.

The flame transfer function is complex; both the magnitude and phase of the heat release response are characterized. The magnitude of the FTF is referred to as "gain" and quantifies the ability of the flame to amplify or damp the normalized velocity oscillation amplitude in the heat release response. The phase of the FTF represents the time delay between velocity oscillations convected into the flame base and corresponding heat release oscillations from the flame.

Flame response is often divided into two regimes: linear and nonlinear. In the linear regime, flame response scales linearly with velocity oscillation amplitude. Therefore, the gain of the flame transfer function in the linear regime is constant. As the amplitude of the velocity oscillation increases, nonlinearities in the flame's heat release response result in saturation and dependence on inlet amplitude (Fig. 2). The illustration represents one possible outcome of nonlinear response: saturation in flame heat release with increasing velocity perturbation magnitude. Response in the nonlinear regime can be irregular and even return to a linear response (see Fig. 11a in the Results and Discussion section).

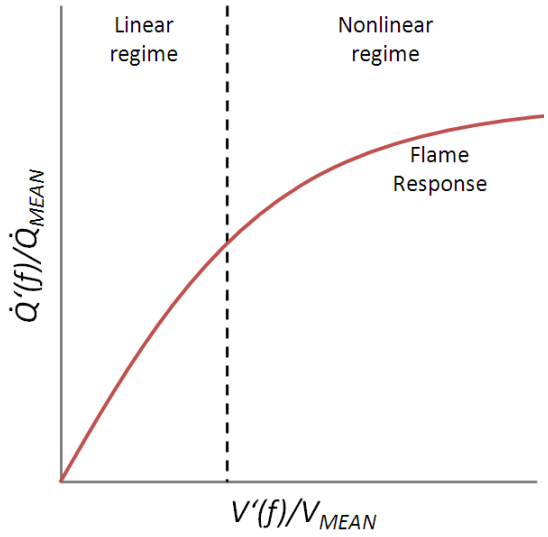

Figure 2. Linear and nonlinear flame response regimes.

Flame Response Literature Review

Merk introduced the concept of a flame transfer function, recognizing the importance of "know[ing] how the fluctuations in heat production depend on the fluctuating conditions of the gas flow" [11]. An analytical model was developed for a multi-component axial combustion system with a conical flame anchored on a burner. The primary focus was to determine the frequencies of excitation where Rayleigh's criterion is satisfied; however, the work did incorporate all important coupling parameters identified in Fig. 1 for a premixed system.

Markstein [12] introduced the transport equation used in analytical (linear form) and computational (nonlinear form) studies. Commonly referred to as the G-equation, the equation describes the motion of an infinitely thin flame front subject to velocity perturbations and is used to model premixed flame response to avoid the difficult and time-consuming task of numerically simulating complete combustion dynamics.

Baillot *et al.* [13] performed one of the earliest experimental flame response studies. A premixed laminar flame was subject to forced flow oscillations and a laser tomography system was used to capture instantaneous images of the unburned gas field seeded with oil. Flame area was determined from the edge of the unburned gas field. The experiments showed the total flame area responded at the frequency of forcing and was deformed by waves propagating through the flame at a speed proportional to the mean flow velocity. In addition, the flame experienced larger relative fluctuations in total area (25%) than velocity fluctuations (10%), indicating the flame is capable of amplifying inlet velocity perturbations.

Candel *et al.* [14] measured the response of a laminar premixed conical flame to small velocity perturbations. PIV measurements in the reactants showed the velocity perturbation traveled downstream at approximately the mean convection velocity. Axial flame cross sections showed large coherent

Copyright © 2011 by ASME

wrinkles generated in the flame front were spaced at convective, not acoustic, wavelengths associated with the mean flow velocity. Comparison between measurements and computations showed that a convective velocity model is necessary for predicting flame response at higher frequencies.

Lieuwen and Neumeier [15] and Bellows *et al*. [16] measured the response of a premixed turbulent flame to velocity oscillations. Analysis of pressure signals acquired at high forcing levels showed nonlinear flame response results from saturation in heat release as acoustic processes remained in the linear regime during limit-cycle instabilities. While liquid and solid rockets experience large relative pressure fluctuations (p'/p_0 ~ 50%) during instability, pressure fluctuations in lean gas turbine systems typically peak at a few percent during limit-cycle operation. Gas dynamic processes remain linear for small pressure fluctuations, as the fluctuations will only have a small effect on the local speed of sound. Dowling [17] showed in a computational study that large velocity and heat release fluctuations are maintained in the presence of small pressure fluctuations.

Research Motivation and Objectives

Self-excited combustion instabilities remain a serious issue hindering the operation of lean, premixed gas turbines. Computational models are necessary in the design and development phase to predict the stability characteristics of specific combustor geometry and operating condition.

Simplified reduced order models are used in predicting the instability characteristics of a combustion system due to the difficult and time-consuming nature of simulating combustion dynamics. Reduced order models divide the overall combustion system into separate elements with individual transfer functions to relate inlet and outlet perturbations. The transfer functions of acoustic elements are approximated based on geometry and mean flow parameters; however, the transfer function of the flame must be empirically measured or modeled using the G-equation [14, 18]. Despite the reliance on flame transfer functions in reduced order models there are no studies directly comparing the heat release response of turbulent premixed flames to velocity perturbations under both self-excited and forced conditions.

The primary objectives of this research are to:

(1) compare self-excited and forced flame response of a turbulent premixed swirl-stabilized flame in both the linear and nonlinear response regimes

(2) characterize the possible mechanisms that result in limit-cycle behavior during self-excited combustion instabilities

EXPERIMENTAL METHODS

Experimental Setup

All measurements are completed in an atmospheric variable-length lean premixed gas turbine research combustor with a single swirl-stabilized industrial injector. Although termed atmospheric, actual mean pressure in the combustor chamber is approximately 1 pisg due to restrictions in the downstream section. An overall view of the experimental setup is provided in Fig. 3. The primary components of the system include an air heater, siren, inlet section, injector, fused-silica combustor, variable-length combustor, and exhaust system. The injector used in this study is a swirl-stabilized industrial injector with a recessed centerbody. The flame is anchored on the outer edge of the centerbody for all operating conditions.

A stainless-steel dump plane is mounted flush with the injector barrel exit. The dump plane is water-cooled to prevent warping and contains an access port for dynamic combustor pressure measurement. An additional port allows access for ignition fuel and high voltage spark igniter used to ignite a diffusion flame used during startup.

A fused-silica tube (inner diameter = 150 mm, wall thickness = 3 mm, length = 305 mm) provides complete optical access for global chemiluminescence emission measurement and flame imaging. The ends of the tube are secured to the dump plane and a water-cooled transition section using high-temperature RTV-silicone. The external surface of the quartz tube is actively cooled with room temperature air supplied by a cooling ring positioned concentric with the tube.

Overall combustor length can be continuously varied between 18 in. and 60 in. using a plug centered in a double-wall

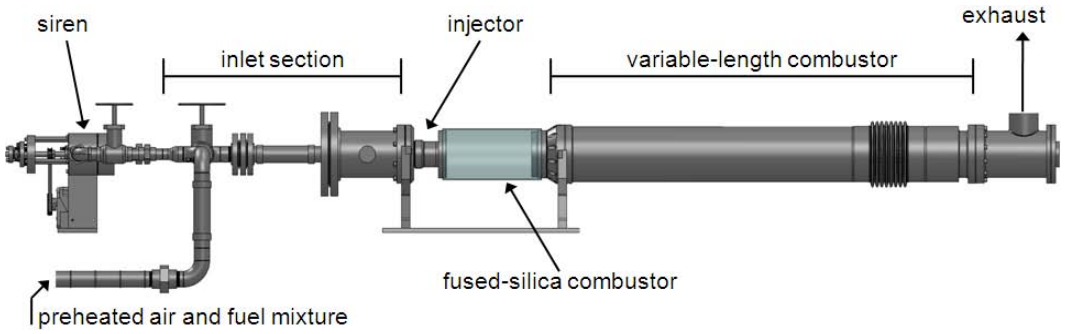

Figure 3. Schematic of overall research combustor. Flow is from left to right.

Copyright © 2011 by ASME

stainless steel combustor section. Changing the combustor length alters the frequency of acoustic modes and mode shape of the overall system. The plug consists of a stainless steel cone cooled using distilled water passed through channels behind the upstream face. The water is then sprayed on the back of the head for additional cooling. Distilled water is used to prevent fouling at high temperatures. A pump elevates the water pressure to approximately 150 psig in the cone to prevent boiling. Combustor length is defined as the distance between the dump plane and base of the cone (Fig. 4).

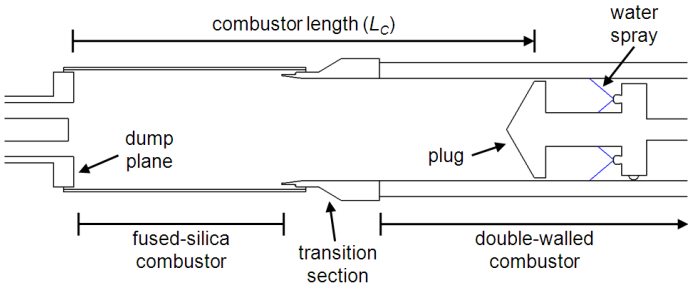

Figure 4. Schematic of fused-silica and variable-length combustors.

A rotor-stator siren is used to modulate the mixture flow during forcing measurements. The rotor is driven by a brushless DC motor. Modulation frequency is set using a digital controller with feedback attached to the DC motor. Feedback keeps the frequency within 1/7 Hz during forcing. The maximum modulation frequency is 500 Hz.

Two globe valves are used to varying the amount of flow through the siren, allowing for control of the modulation level (Fig. 5). In general, the maximum achievable modulation level decreases with increasing modulation frequency.

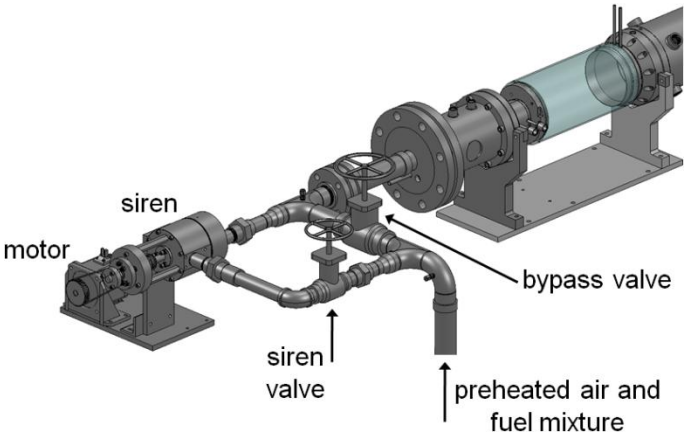

Figure 5. Description of air-fuel mixture forcing system.

Data Acquisition and Instrumentation

Dynamic pressure and global chemiluminescence signals are recorded nearly simultaneously (one microsecond delay between each data point acquisition). All signals are recorded with a sampling rate of 8192 samples/seconds for 32 seconds. The records are divided into 32 one-second long records and analyzed separately, leading to a frequency resolution of 1 Hz.

Dynamic pressure measurements serve two primary purposes: characterize the magnitude of self-excited combustion instabilities (combustor pressure transducer) and provide pressure fluctuations needed to calculate particle velocity fluctuations using the two-microphone method (upstream and downstream transducers). All transducers are water cooled and recessed mounted to prevent overheating. The charge output of each transducer is converted to voltage with an inline converter and amplified by a factor of ten.

An accurate measurement of heat release is needed to quantify the flame's response to velocity and equivalence ratio perturbations. Global chemiluminescence emission has been used in numerous flame studies, based on experiments that show that for a fixed equivalence ratio, global chemiluminescence is directly proportional to fuel mass flow [19-21]. In this study, CH* chemiluminescence emission is measured using a photomultiplier tube (PMT) with a 432 ± 5 nm band-pass filter. In addition to simplicity, global chemiluminescence has shown good agreement with more detailed local measurements of flame heat release [22].

Particle velocity fluctuations near the base of the flame must be determined to provide an input fluctuation (V'_{RMS}) for the premixed flame transfer function. Several methods exist to measure particle velocity, including hot-wire anemometry (HWA) and laser-doppler velocimetry (LDV). HWA cannot be used due to the elevated inlet mixture temperature (> 200 C) and LDV would require additional optical access in the injector barrel and seeding. In addition, both HWA and LDV provide point velocity measurements while the mean axial velocity fluctuation is needed. To eliminate the problems associated with HWA and LDV, the two-microphone method is used to calculate particle velocity fluctuations from dynamic pressure measurements [23].

Data Analysis Procedures

Signal Analysis:

Pressure, velocity, and chemiluminescence signals are analyzed in the frequency-domain to characterize response at or near the perturbation frequency. A Fast-Fourier Transform (FFT) is used to calculate a signal's linear spectrum. The phase of the perturbation is determined from the angle between the real and imaginary component of the linear spectrum. The signal's single-sided power spectral density (SSPSD) is then calculated from the linear spectrum and Parseval's theorem is used to calculate fluctuation magnitudes. Parseval's theorem relates the root-mean-square (RMS) energy of a signal in the

Copyright © 2011 by ASME

frequency-domain to the RMS energy of a signal in the time-domain [24]:

$$rms(i) = \sqrt{G_{xx}(i) \cdot \Delta f} \qquad (2)$$

where i is the bin number of the frequency of interest, $rms(i)$ is the corresponding time-domain RMS magnitude, $G_{xx}(i)$ is the corresponding frequency-domain SSPSD value, and Δf is the frequency resolution.

Comparison between Self-excited and Forced Signal Analysis:

During forcing measurements, the frequency of the velocity perturbations generated by the siren are controlled to within a fraction of a hertz using the controller with feedback described in the Experimental Setup section. However, during self-excited measurements, an unstable flame couples with system acoustics and the dominant frequency of self-excited oscillations must be determined from pressure, velocity, or chemiluminescence spectra. To account for uncertainty in the exact frequency of oscillation, Parseval's theorem is used across a range of frequencies near the peak frequency to better represent the oscillation magnitude:

$$rms(i) \approx \sqrt{\sum_{i=-5\,Hz}^{i=+5\,Hz} G_{xx}(i) \cdot \Delta f} \qquad (3)$$

If the oscillation frequency does not correspond to the center bin frequency, energy will spread to nearby bins as a result of the analysis procedure (leakage). In addition, the actual oscillation frequency is most likely not constant during the time required to record a signal, resulting in energy spread throughout several bins. During the forcing measurements oscillation frequency is held nearly constant using a controller with feedback that maintains the forcing frequency to within 1/7 Hz.

Fig. 6 shows an example of a typical SSPSD of self-excited and forced flame CH* chemiluminescence signals. Pressure and velocity SSPSDs are similar. The self-excited SSPSD (a) shows the 171 Hz bin contains the greatest energy, with some energy spread to nearby bins. The forced SSPSD (b) shows almost all energy is contained within the bin corresponding to the forcing frequency (170 Hz). Summing the energy of bins within ±5 Hz of the dominant frequency results in similar CH* chemiluminescence fluctuation magnitudes.

Uncertainty in Linear Regression Analysis:

Linear regression is used to find the slope of the line of best fit through zero to determine the gain of each data set. The uncertainty in the slope is calculated using a method that relates the coefficient of determination (R^2) of a linear regression fit to the relative uncertainty in the slope [25]:

$$\frac{\sigma(a)}{|a|} = \frac{\tan\left(a\cos\left(\sqrt{R^2}\right)\right)}{\sqrt{N-2}} \qquad (4)$$

where N is the number of data points, a is the slope of the line of best fit, and $\sigma(a)$ is the absolute uncertainty in the slope.

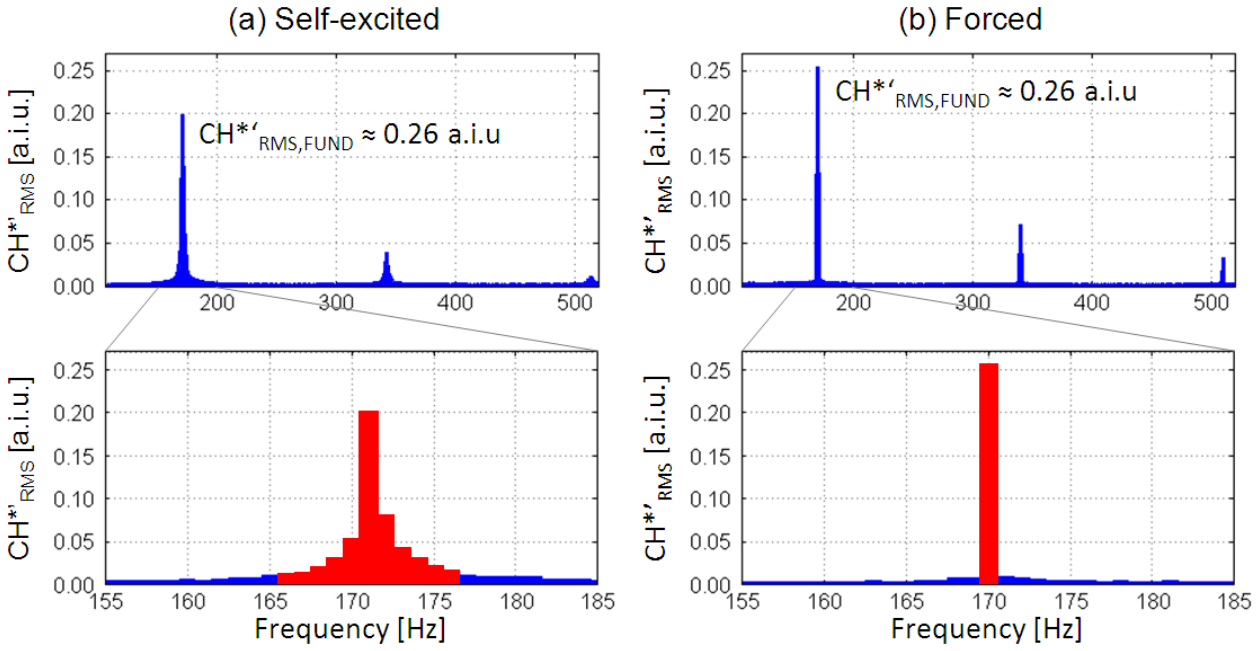

Figure 6. Example CH* chemiluminescence SSPSDs for self-excited and forced flames (operating condition: premixed natural gas and air, T_{IN} = 250 C, v_{MEAN} = 40 m/s, Φ = 0.65, v'/v_{MEAN} = 0.10).

Copyright © 2011 by ASME

RESULTS AND DISCUSSION

Linear Flame Response Regime

Under self-excited operation the dynamics of an unforced flame are characterized by varying the combustor length (L_C) and measuring the corresponding combustor pressure oscillation magnitude and frequency. Fluctuations in velocity and heat release result from coupling between flame heat release and system acoustics at the instability frequency; the flame's response is quantified using the same FTF concept used to describe forced flame response (Eq. 1).

For the first operating condition in this study (natural gas, T_{IN} = 250 C, V_{MEAN} = 40 m/s, Φ = 0.65) self-excited instabilities were observed over a combustor length range of 18 – 22 in. The instability frequencies vary between 165 and 170 Hz due to the slight change in combustor length and correspond to a longitudinal mode associated with the overall combustor geometry. Forcing measurements were then completed to compare self-excited and forced flame response at 170 Hz. Three combustor lengths were chosen (27, 35, and 55 inches) where the flame is stable and the forcing measurement was repeated at 170 Hz with varying velocity perturbation levels.

Fig. 7 shows a comparison of the self-excited and forced flame response. Fig. 7(a) shows the normalized global heat release (CH*) fluctuation versus inlet velocity fluctuation at the fundamental perturbation frequency. Fig. 7(b) shows the phase difference between velocity and heat release perturbations, which is equivalent to the phase of the flame transfer function. Coherence values between velocity and heat release at the fundamental frequency are shown in Fig. 7(c).

In the linear regime, the slope of a line through each data set is equivalent to the gain of the flame transfer function. Uncertainty in the gain was determined using the method described in the Experimental Methods section. Table 1 shows all measurements of the flame response gain within the limits of uncertainty, indicating that the forcing measurement provides an accurate measurement of flame response amplitude to velocity perturbation.

Table 1. Flame response magnitude comparison between forced and self-excited measurements.

		L_C [in.]	Gain	Uncert.	Range
●	Forced 1	27	1.13	4.6%	1.08 – 1.18
♦	Forced 2	35	1.09	4.2%	1.04 – 1.14
▲	Forced 3	55	1.06	2.7%	1.03 – 1.09
■	Self-excited	18 – 22	1.07	3.2%	1.04 – 1.10

In addition, a comparison of the phase difference between velocity and heat release fluctuations for all four data sets shows good agreement; the largest difference between self-excited and forced measurements is approximately 13° or 4% of one cycle. The phase difference corresponds to the time delay between velocity perturbations in the injector and heat release perturbations from the flame. Since the mean flow velocity was held constant in all measurements, the agreement between the self-excited and forced measurements indicates the distance the velocity perturbation traveled to generate a heat release perturbation remained constant, i.e. no large variations in flame position occur between self-excited and forced measurements. Finally, coherence at the perturbation frequency is excellent (>0.98) for all forcing measurements and remains above 0.94 during all self-excited measurements, indicating

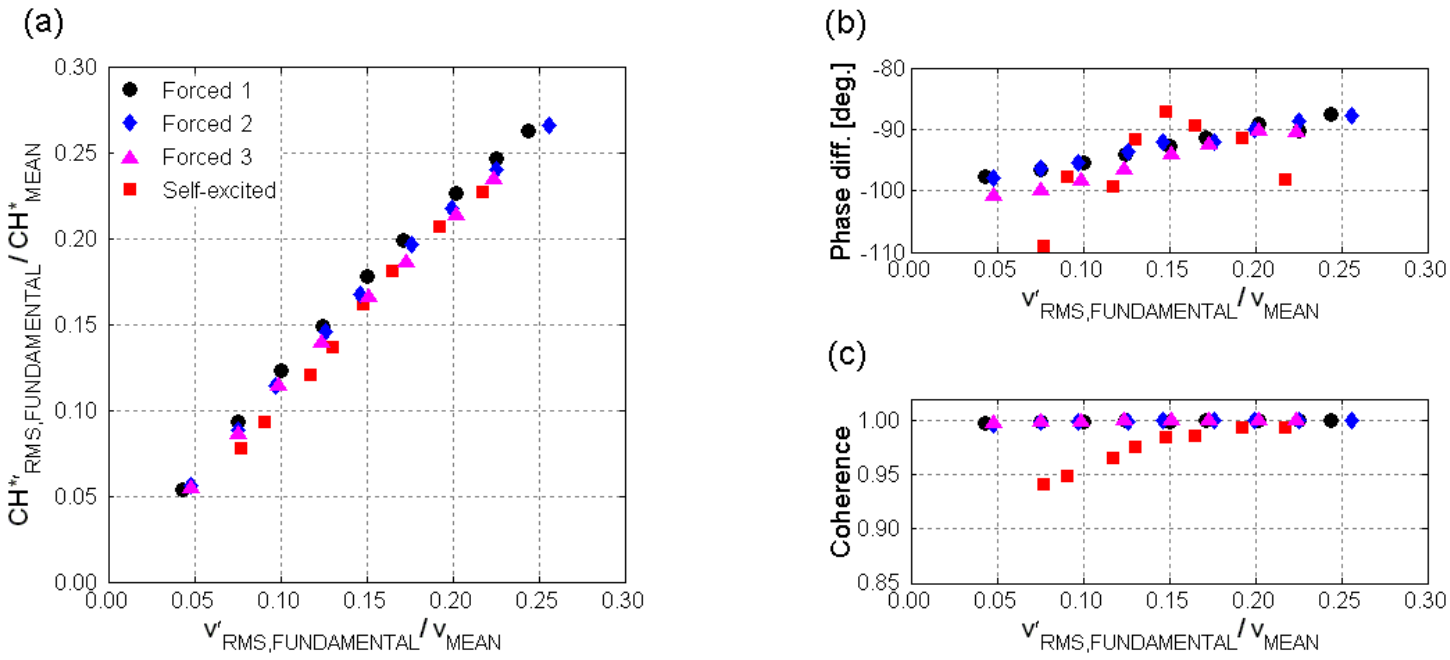

Figure 7. Normalized flame response (a), phase difference (b), and coherence (c) between CH*' and v' for both self-excited and forced flames (operating condition: premixed natural gas and air, T_{IN} = 250 C, v_{MEAN} = 40 m/s, Φ = 0.65).

Copyright © 2011 by ASME

high correlation between velocity and heat release perturbations.

The first part of this section compares flame response between self-excited and forced measurements. However, the overall system response changes with combustor length and provides additional insight to the combustion instability feedback process. The effect of changing combustor length on the relationship between combustor pressure and velocity fluctuation magnitude is shown in Fig. 8.

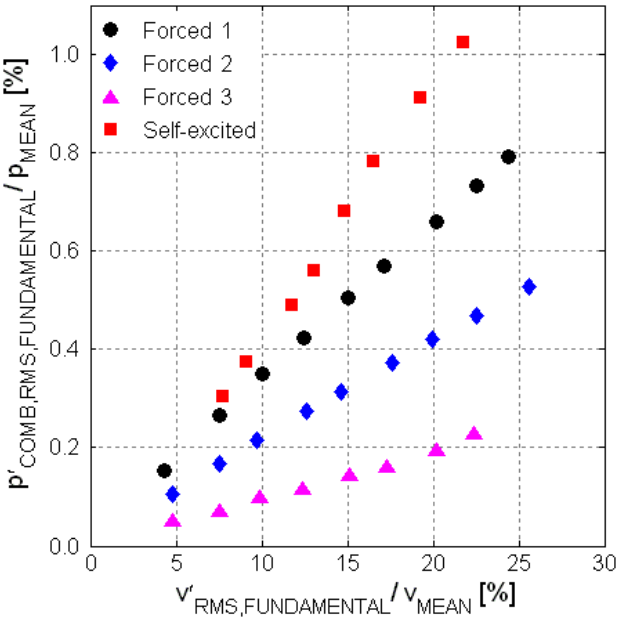

Figure 8. Combustor pressure fluctuation magnitude comparison between self-excited and forced flames.

In general, the magnitude of the combustor pressure oscillation is larger during self-excited unstable flame measurements than forced flame unstable measurements due to the positive coupling between heat release/pressure (Rayeigh's criterion) necessary for maintaining the feedback cycle. Forcing measurements were completed at stable combustor lengths; therefore, heat release and pressure fluctuations must be out of phase or pressure perturbations must be sufficiently damped at these lengths to prevent feedback resulting in an unstable flame.

Fig. 9 shows the phase difference between combustor pressure and heat release. In the self-excited and first two forced cases, Rayleigh's criterion for positive coupling between heat release and pressure is satisfied. This indicates that the heat release process is adding energy to the acoustic field, increasing the combustor pressure magnitude. Since the first two forcing cases were completed at stable lengths, acoustic pressure fluctuations generated by heat release from the flame must be sufficiently damped to prevent self-excited instability. In the third forcing case, heat release and pressure are out of phase and heat release perturbations from the flame damp the acoustic pressure field.

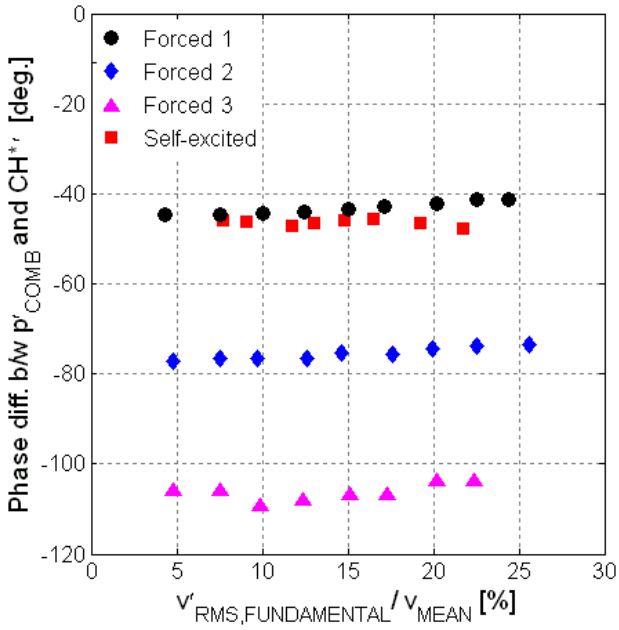

Figure 9. **P**hase difference between combustor pressure and heat release (Rayleigh's criterion) comparison between self-excited and forced flames.

Figures 8 and 9 also indirectly show that flame response cannot be characterized through a pressure-heat release relationship as the magnitude of the pressure fluctuation changes but the flame response remains constant. The underlying mechanism that relates velocity perturbations to heat release perturbations in lean premixed flames shows that pressure exerts a minimal effect on flame response. In a lean premixed flame heat release is directly proportional to the mass flow of fuel entering the flame front. The flame's rate of heat release does not respond directly to velocity fluctuations, but to fuel mass flow rate fluctuations directly generated by velocity fluctuations:

$$v' \rightarrow \dot{m}_{FUEL}{}' \rightarrow q'$$

Fuel mass flow rate can also fluctuate due to pressure fluctuations through changes in mixture density:

$$p' \rightarrow \rho' \rightarrow \dot{m}_{FUEL}{}' \rightarrow q'$$

However, in lean premixed gas turbine combustion, pressure fluctuations are typically an order of magnitude smaller than velocity fluctuations. For the operating condition tested, the maximum pressure fluctuation is p'_{RMS}/p_{MEAN} ~ 1% while the maximum velocity fluctuation is V'_{RMS}/V_{MEAN} ~ 25%.

Copyright © 2011 by ASME

Finally, based on the linear response of the flame, the limit-cycle behavior of self-excited flames at this operating condition cannot be attributed to saturation in flame response. Fig. 10 depicts the interaction of driving (flame response) and damping processes in the combustor leading to limit-cycle oscillation. Most combustion instability models assumed saturation in flame response as the nonlinear mechanism limiting oscillation magnitude (top). The self-excited and forced flame response provided in the previous section show limit cycle behavior in the linear flame response regime, indicating that nonlinearities in damping limit oscillation magnitude in this case (bottom).

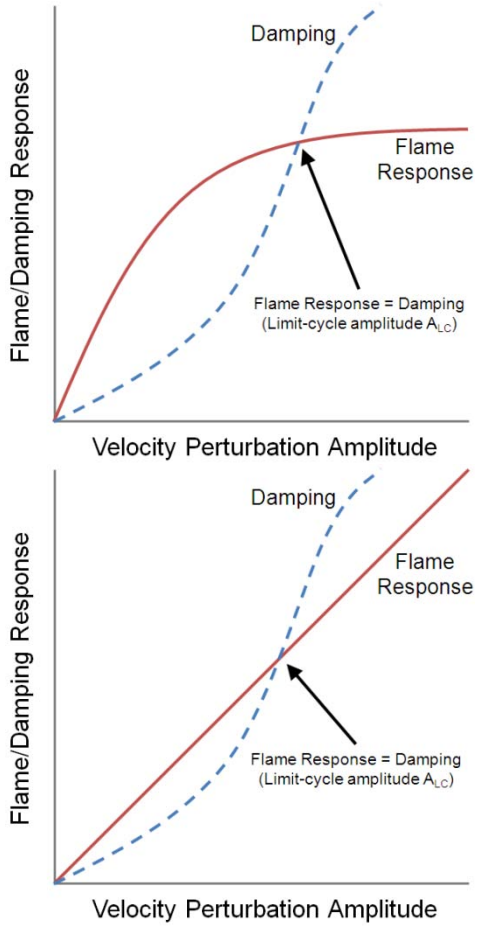

Figure 10. Depiction of flame response and damping mechanism interaction leading to limit-cycle oscillation. Top: saturation in flame response limits oscillation magnitude. Bottom: nonlinear system damping limits oscillation magnitude (modified from [9]).

Nonlinear Flame Response Regime

The second operating condition (natural gas, T_{IN} = 250 C, v_{MEAN} = 40 m/s, Φ = 0.525) tested during this study produced a nonlinear flame response in both self-excited and forced experiments. The measurement procedure was identical to the procedure used in the previous section. During self-excited measurements, the frequency of the oscillations varied between 150 and 160 Hz due to the change in combustor length over a short distance. Two forcing measurements were completed at the two bounding frequencies after the combustor was tuned to a stable flame operating length: 150 Hz (Forced 1) and 160 Hz (Forced 2).

Fig. 11 shows a comparison of the self-excited and forced flame response. Fig. 11(a) shows the normalized global heat release (CH*) fluctuation versus inlet velocity fluctuation at the fundamental oscillation frequency. Flame response is linear through $V'_{RMS}/V_{MEAN} \approx 0.25$ for both self-excited and forced measurements but starts to saturate with increasing velocity fluctuation magnitude. The largest observed self-excited velocity fluctuation was $V'_{RMS}/V_{MEAN} \approx 0.42$. All values of self-excited and forced flame response at each velocity fluctuation magnitude agree within uncertainty.

The largest velocity fluctuation achieved during self-excited experiments is determined by the feedback loop detailed in Fig. 1. The forced response experiment "breaks" the feedback cycle dependency allowing for more control of the velocity fluctuation magnitude. The maximum velocity fluctuation magnitude was extended up to $V'_{RMS}/V_{MEAN} \approx 0.6$ using the siren to characterize flame response past the range achieved during self-excited measurements. Although the heat release response starts to saturate after $V'_{RMS}/V_{MEAN} \approx 0.25$, the forcing measurements show the flame response starts to increase again with increasing velocity fluctuation magnitude past $V'_{RMS}/V_{MEAN} \approx 0.45$.

At this operating condition, self-excited flame response exhibited both linear ($V'_{RMS}/V_{MEAN} < 0.25$) and nonlinear ($V'_{RMS}/V_{MEAN} > 0.25$) behavior. For conditions in the linear regime, the final limit cycle amplitude was restricted by nonlinearities in damping (Fig. 10 Bottom). However, this operating condition also shows saturation behavior in flame response (Fig. 10 Top) resulting in limit-cycle behavior.

Copyright © 2011 by ASME

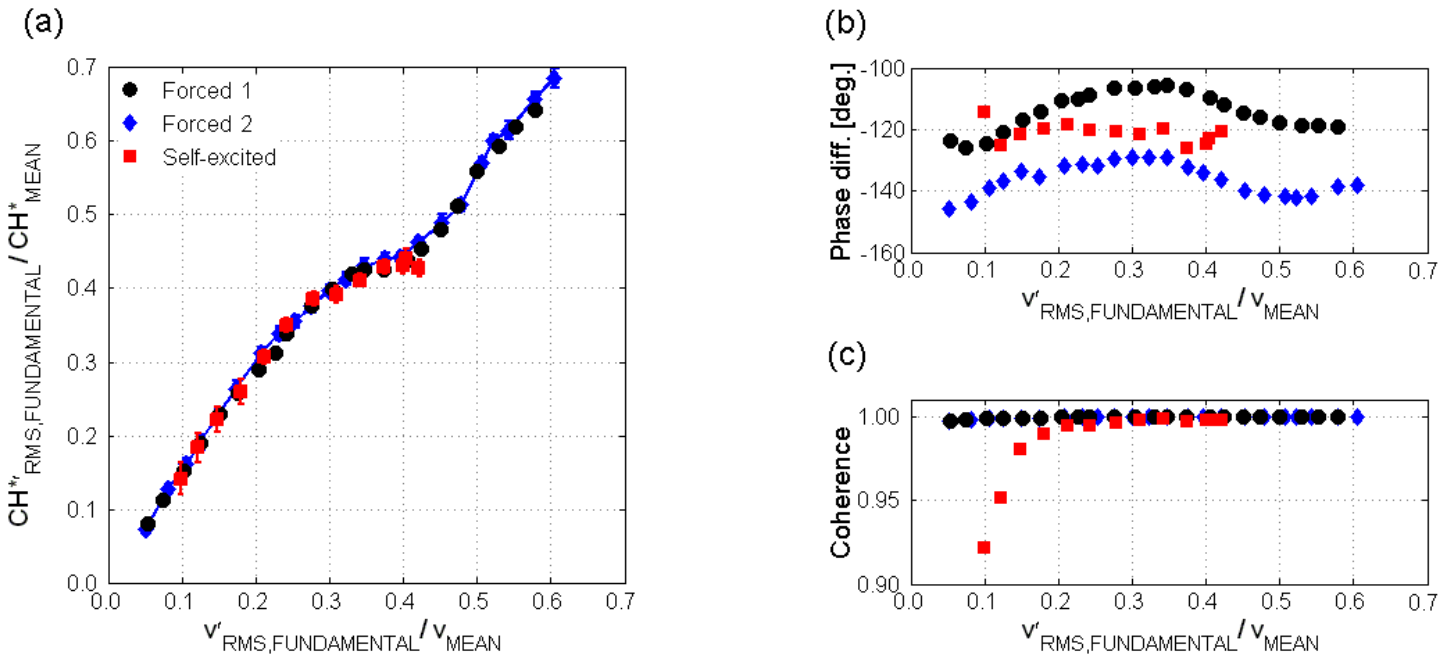

Figure 10. Normalized flame response (a), phase difference (b), and coherence (c) between CH*' and v' for both self-excited and forced flames (operating condition: premixed natural gas and air, T_{IN} = 250 C, v_{MEAN} = 40 m/s, Φ = 0.525).

CONCLUSION

Flame response measurements presented show that premixed flame response to single frequency velocity perturbations is identical for both self-excited and forced flames at the same operating condition. In lean premixed flames, velocity perturbations produce fuel mass flow perturbations, which generate heat release perturbations from the flame. Pressure fluctuations exert minimal influence on flame response in typical gas turbine systems due to the relatively low pressure fluctuation level and long acoustic wavelength at low frequencies. Flame response measured during the forcing measurement captures the transition to the nonlinear region also observed in self-excited measurements. Finally, linearity in flame response observed during self-excited measurements indicates nonlinear damping mechanisms may result in the limit-cycle behavior of combustion instabilities and must be accounted for in reduced order modeling.

ACKNOWLEDGMENTS

The research presented in this paper was supported by Solar Turbines, Inc.

REFERENCES

[1] US DOE/EIA, 2010, "Annual Energy Outlook 2010 - With Projections to 2035."
[2] Walsh, P. P., & Fletcher, P., 2004, *Gas Turbine Performance* (2nd Edition), Blackwell Science Ltd., Oxford, United Kingdom, Chap. 8.
[3] US DOE/EIA, 2010, "Electric Power Annual 2008."
[4] US EPA, 1993, "Alternative Control Techniques Document - NOx Emissions from Stationary Gas Turbines."
[5] Kinsler, L. E., Frey, A. R., Coppens, A. B., and Sanders, J. V., 2000, *Fundamentals of Acoustics* (4th Edition). John Wiley & Sons, Inc., United States, Chap. 5.
[6] Lieuwen, T. C., and McManus, K., 2003, "Introduction: combustion dynamics in lean-premixed prevaporized (LPP) gas turbines," Journal of Propulsion and Power, **19**(5), p. 721.
[7] Huang, Y., and Yang, V., 2009, "Dynamics and stability of lean-premixed swirl-stabilized combustion," Progress in Energy and Combustion Science", **35**, pp. 293-364.
[8] Keller, J. J., 1995, "Thermoacoustic oscillations in combustion chambers of gas turbines," AIAA Journal , **33**(12), pp. 2280-2287.
[9] Zinn, B. T., and Lieuwen, T. C., 2005, "Combustion Instabilities: Basic Concepts," In B. T. Zinn, & T. C. Lieuwen (Eds.), *Combustion Instabilities in Gas Turbine Engines*, pp. 3-24.
[10] Rayleigh, L., 1878, "The explanation of certain acoustic phenomena," Nature, **18**, pp. 317-319.

Copyright © 2011 by ASME

[11] Merk, H., 1957, "An analysis of unstable combustion of premixed gases," Symposium (International) on Combustion, **6**, pp. 500-512.
[12] Markstein, G., 1964, "Theory of Flame Propagation," In G. Markstein, *Non-steady Flame Propagation.*
[13] Baillot, F., Durox, D., and Prud'homme, R., 1992, "Experimental and theoretical study of a premixed vibrating flame," Combustion and Flame, **88**, pp. 149-168.
[14] Schuller, T., Ducruix, S., Durox, D., and Candel, S., 2002, "Modeling tools for the prediction of premixed flame transfer functions," Proceedings of the Combustion Institute, **29**, pp. 107-113.
[15] Lieuwen, T., and Neumeier, Y., 2002, " Nonlinear pressure-heat release transfer function measurements in a premixed combustor," Proceedings of the Combustion Institute, **29**, pp. 99-105.
[16] Bellows, B. D., Neumeier, Y., and Lieuwen, T., 2006, "Forced response of a swirling, premixed flame to flow disturbances," Journal of Propulsion and Power, **22**, pp. 1075-1084.
[17] Dowling, A., 1997, "Nonlinear self-excited oscillations of a ducted flame," Journal of Fluid Mechanics, **346**, pp. 271-290.
[18] Shanbhogue, S., Shin, D.-H., Hemchandra, S., Plaks, D., and Lieuwen, T., 2009, "Flame sheet dynamics of bluff-body stabilized flames during longitudinal acoustic forcing," Proceedings of the Combustion Institute, **32**, pp. 1787–1794.
[19] Diederichsena, J., and Goulda, R., 1965, "Combustion instability: Radiation from premixed flames of variable burning velocity," Combustion and Flame, **9**(1), pp. 25-31.
[20] Pricea, R., Hurlea, I., and Sugdena, T., 1969, "Optical studies of the generation of noise in turbulent flames," Symposium (International) on Combustion, **12**(1), pp. 1093-1102.
[21] Lee, J., and Santavicca, D., 2003, "Experimental diagnostics for the study of combustion instabilities in lean premixed combustors," Journal of Propulsion and Power, **19**(5), pp. 735-750.
[22] Balachandran, R., Ayoola, B., Kaminski, C., Dowling, A., and Mastorakos, E., 2005, "Experimental investigation of the nonlinear response of turbulent premixed flames to imposed inlet velocity oscillations," Combustion and Flame, 143, pp. 37-55.
[23] Waser, M. P., and Crocker, M. J., 1984, "Introduction to the two-microphone cross-spectral density method of determining sound intensity," Noise Control Engineering, **22**(3), pp. 76-85.
[24] Mitra, S. K., 2006, *Digital Signal Processing (3rd Edition).* McGraw-Hill., United States, Chap. 4.
[25] Higbie, J., 1991, "Uncertainty in the linear regression slope," American Journal of Physics, **59**(2), pp. 184–185.

 Copyright © 2011 by ASME